Revisiting the application of molecular probe diagnostics on quantifying aqueous OH radicals in plasma-liquid systems

Qingjin Tang[1], Mingjia Zhang[1], Binhong Wu[1], Xin Wang[1], Xin Tu[2], Kostya (Ken) Ostrikov[3] Linsheng Liu[4], and Qiang Chen[*,1]

[1]*Fujian Provincial Key Laboratory of Plasma and Magnetic Resonance, Fujian Provincial Key Laboratory of Electromagnetic Wave Science and Detection Technology, Xiamen Key Laboratory of Multiphysics Electronic Information, Institute of Electromagnetics and Acoustics, Xiamen University, Xiamen 361005, China*

[2]*Department of Electrical Engineering and Electronics, University of Liverpool, Liverpool L69 3GJ, UK*

[3]*School of Chemistry and Physics and QUT Centre for Materials Science, Queensland University of Technology (QUT), Brisbane, QLD 4000, Australia*

[4]*School of Electronic and Information Engineering/School of Integrated Circuits, Guangxi Normal University, Guilin 541004, China*

[*]*Email: chenqiang@xmu.edu.cn*

Abstract:

We revisit one of the most used techniques for quantifying the aqueous *OH* radicals (OH_{aq}) in plasma-liquid systems, the molecular probe method which obtains the [OH_{aq}] through measuring a stable material formed by a rapid reaction between the molecular probe and the OH_{aq}. In this study, we used *NaTA* as the molecular probe, the experimental results with a theoretical analysis suggest that to obtain the correct OH_{aq} concentration, the concentration of molecular probe should be greater than a certain

value which depends on the types of the plasma-liquid systems. However, this is not the case in most of the existing reports in which the *NaTA* are often much less than the requisite value.

Keywords: Plasma-liquid interactions; molecular probe; hydroxyl radical; fluorescence

1. Introduction

If a sufficient amount of electrical energy is input to a gas, the gas can be ionized to form a discharge plasma which is composed of energertic electrons, ions, reactive and radical species. The dischage plasma is highly reactive so that it can be used across several fields [1, 2]. A contact of a gaseous plasma with a liquid creates a gas-liquid interface, through which charge and mass are transferred between the plasma and the liquid [3-6]. Consequently, the liquid is activated and the plasma reactivity turns into the reactivity of the liquid. The reactivity transfer involves many phyical, chemical, and electrochemical processes which can generate plentiful reative species. The reative species can be categorized into long- and short-lived species depending on their reactivity [7-12]. Hydrogen peroxide (H_2O_2) and hydoxyl (*OH*) are two typical long-lived and short-lived reactive species, respectively, commonly generated when dischage plasmas are in contact with auqeous solutions. The *OH* radicals are very important in applications of plasma-liquid systems such as water treatment [13-15] and plasma medicine [16-21]. Therefore, measuring the concentrations and understanidng the mechanisms of the *OH* radical formation in plasma-treated solutions is crucial.

The redox poential of the *OH* radical is as high as 2.85 eV *vs* standard hydrogen electrode [22], which makes the *OH* radical highly reactive. A weak absportion band below 300 nm for the *OH* radical was observed in an aqueous solution [23, 24]. However, a direct method using this absportion band to quantify the *OH* radical is is challenging due to its short lifetime (~ μs) [25] as well as the

possible interference with other substances' absorption within this band. Therefore, many existing measurements rely on indirect methods. The molecular probe diagnostics is one of the commonly used indirect methods. The molecular probe measurements are based on the following process. A substance called molecular probe, can selectively react with *OH* radical to form a stable product at a high reaction rate (Eq. 1). Since the product is relatively stable, one can quantify the product and then deduce the concentration of the *OH* radical. In most plasma-liquid systems, researchers measured the concentration of the product, and then directly deduced the *OH* concentration. However, this process involves some ambiguity, hence some concepts and the measurement results should be clarified. In this paper, we revisit the molecular probe method and clarifythe key concepts in the measurements, such as the influence of the molecular probe concentration and clarify the meaning of the conventionally measured values of *OH* concentration. Following the discussions in [26], we present the details about the molecular probe diagnostics method as follows.

Assuming that a discharge plasma is in contact with an aqueous solution containing a substance (*S*, a *OH* molecular probe) and some other unknown *OH* scavengers *X* (*X* represents a group of unknown substances). To study the OH consumption, one must track the rapid reactions related with the *OH* radicals. Besides *S* and *X*, the OH itself is also an important reactant able to rapidly react with itself, and as a result, the *OH* radicals formed in the plasma-treated solution can be rapidly consumed by Eqs. 1-3,

$$OH + S \rightarrow OH^- + S^+ \quad (1)$$

$$OH + OH \rightarrow H_2O_2 \quad (2)$$

$$OH + X \rightarrow OH^- + X^+, \quad (3)$$

where Eqs. 1 and 3 are just one type of possibile reactions, because in some cases the reactions might be the addition, hydrogen abstraction, and radical interaction processes rather than an electron transfer

reaction [27].

Based on these reactions, the variation of the *OH* concentration with respect to time (d[*OH*]/dt) and the production rate of [S^+] ($G_{[S+]}$) in the solution can be expressed as

$$\frac{d[OH]}{dt} = G_{[OH]_g} - k_1[OH][S] - k_2[OH]^2 - k_3[OH][X] \qquad (4)$$

$$G_{[S^+]} = \frac{d[S^+]}{dt} = k_1[OH][S]. \qquad (5)$$

where $G_{[OH]g}$ is the rate cahnge of the OH concentration in the plasma-treated solution, if all the dissolved gaseous OH radicals are not consumed. k_1, k_2 and k_3 are the rate constants of Eqs. 1-3, respectively. In this paper, all the concentrations without a subscript represent pseudo steady states.

Because of its very strong reactivity, the *OH* radical in the solution should be in a pseudo steady state (d[*OH*]/dt=0, here [*OH*] being a small constant due to its high reactivity), then

$$G_{[OH]_g} = k_1[OH][S] + k_2[OH]^2 + k_3[OH][X]. \qquad (6)$$

Combining Eq. 5 with Eq. 6, we have

$$\frac{1}{G_{[S^+]}} = \frac{1}{G_{[OH]_g}}\left\{\frac{\frac{k_2}{k_1}[OH] + \frac{k_3}{k_1}[X]}{[S]} + 1\right\}. \qquad (7)$$

If $\{k_2[OH] + k_3[X]\}/k_1$ is assumed to be a constant A, we then obtain

$$\frac{1}{G_{[S^+]}} = \frac{1}{G_{[OH]_g}}\left\{\frac{A}{[S]} + 1\right\}. \qquad (8)$$

There should be a linear relationship between $1/G_{[S+]}$ and $1/[S]$, and $G_{[OH]g}$ might be estimated from the curve of $1/G_{[S+]}$ *vs* $1/[S]$ (by calcualting its intercept, $1/G_{[OH]g}$). Moreover, if [*S*] is much greater than *A*, *A*/[*S*] will be close to zero, and consequently the value of $1/G_{[OH]g}$ will be close to $1/G_{[S+]}$.

Based on the above description, the concentrations of the plasma-generated *OH* {$[OH]_g$ and the pseudo steady state *OH* {[*OH*]} species in the solution are

$$[OH]_g = \int G_{[OH]_g} dt \quad (9)$$

$$[OH] = \frac{G_{S^+}}{k_1[S]}. \quad (10)$$

If the conversion ratio of *OH* to S^+ is α, the measured concentration of the *OH* radicals in the plasma-treated solution, $[OH]_m$, is usually expressed in most previous studies as Eq. 11

$$[OH]_m = [S^+]/\alpha = \int G_{[S^+]} dt/\alpha = \int k_1[OH][S]dt/\alpha. \quad (11)$$

It is worth noting that $[OH]_m$ is a function of [*S*] and it increases with increasing [*S*]. However, this fact is not paid due attention in many cases. For convenience, in Table 1, we summarize the typical notations and their meaings used in this paper.

Table 1. Notations used in this paper and their meanings.

Notation	Meaning
[*OH*], [*S*], [*X*], [S^+]	Steady state concentrations of *S*, *OH*, *X* & S^+
$G_{[OH]g}$	Change rate of the [*OH*] in the plasma-treated solution, if all dissolved gasoues OH are not consumed
$G_{[S+]}$	Production rate of [S^+] in the solution
$[OH]_g$	Plasma-generated *OH* in the solution
$[OH]_m$	Measured *OH* concentration in the plasma-treated solution in most studies

In this paper, using disodium terephthalate (*NaTA*) as the molecular probe, we demonstrate that the quantification of *OH* radicals in a plasma-treated aqueous solution is complex and due attention should be paid to the exact meaning of the measured results.

2. Experimental setup

Figure 1(a) illustrates the experimental setup. Ar (40 sccm) is supplied through the hollow tungsten steel electrode (slightly tapered at the nozzle, 1.02 mm in inner and 6.35 mm in out-side diameters). Ar discharge is ignited by a DC power source (TESLAMAN TRC2025N20-1000) between a flowing aqueous solution and the hollow tungsten steel electrode. Inset of Fig. 1(a) gives a photograph of the discharge plasma. A graphite rod is submerged in the solution to conduct the circuit. The discharge gap and current are 3 mm and 40 mA, respectively. To avoid a glow-arc transition, a ballast resistor

(100 kΩ) is connected in series in the circuit. The discharge current is measured by dividing the voltage across a 10-Ω ballast resistor. The solution (50 ml, 100 ml/min) is pushed through a polytetrafluoroethylene cylindrical reactor by a peristaltic pump (Runze Fluid YZ1515X). After the plasma treatment, the solution enters a cooling bottle (25 °C), and then passes through a quartz flow-through cuvette with an optical path of 10 mm, and finally enters the cylindrical reactor.

NaTA is a well-known *OH* scavenger and it can react with OH very quickly to form some products, and one of the products is 2-hydroxyterephthalic acid (*HTA*). *HTA* molecule can emit a fluorescent light at 425 nm when it is irradiated by a UV−light with a wavelength at 310 nm. The intensity of the fluorescent light for *HTA* is independent of pH value in the range of pH 6-11 [28]. Therefore, a phosphate-buffered solution (PBS, pH 7.0, buffer strength 10 mM) containing disodium terephthalate (*NaTA*) is used as the plasma-treated aqueous solution.

The discharge voltage between two electrodes (V_d) is measured by a high volage probe (Tektronix P6015A) connected with the two electrodes, and the discharge power (P_d) is estimated by multiplying the discharge current with V_d. The measured power equals the addition of the powers consumed by the plasma and by the solution zone between the plasma and the bottom electrode. Table 2 presents the discharge information we used in the experiment. We can find that for a fixed discharge current of 40 mA, the power ranges from 27.2 W to 47.6 W and decreases with increasing NaTA concentration. This can roughly attributed to the decrease of power consumed by the solution between the plasma and the bottom electrode, since the resistance of this solution zone decreases with increasing NaTA concentration.

Table 2. The discharge voltage between two electrodes (V_d) and the discharge powers (P_d) for the plasma-liquid system with different *NaTA* concentrations ([NaTA]). The discharge current is 40 mA.

[NaTA] (mM)	V_d (kV)	P_d (W)
2.00	1.19	47.6

5.0	1.08	43.2
12.5	0.97	38.8
25.0	0.88	35.2
50.0	0.81	32.4
75.0	0.73	29.2
100.0	0.73	29.2
150.0	0.71	28.4
200.0	0.68	27.2

Figure 1(b) presents the Y-type reflection optical fiber probe used to detect the fluorescent light. A light with a wavelength of 310±5 nm (from a LED light source, JINGYI)) is guided to the quartz cuvette wall by the irradiation optical fibers (a bunddle of six optical fibers), and the HTA is excited to irradiate fluorescent light at the quartz cuvette wall. The reflected fluorescent light on the quartz cuvette wall is then guided to the spectrometer end through the recording optical fiber, and then recorded by a USB6500-Pro spectrometer (JINGYI).

NaTA (>99.0%) was purchased from Shanghai Yuanye Bio-Technology Co., Ltd, *HTA* (98.0%) was purchased from Shanghai Aladdin Biochemical Technology Co., Ltd, and monosodium phosphate (⩾99.0%) and sodium hydrogen phosphate (⩾99.0%) were provided by Xilong Scientific Co., Ltd. and Sinopharm Chemical Reagent Co., Ltd., respectively. All chemicals were used without further treatment.

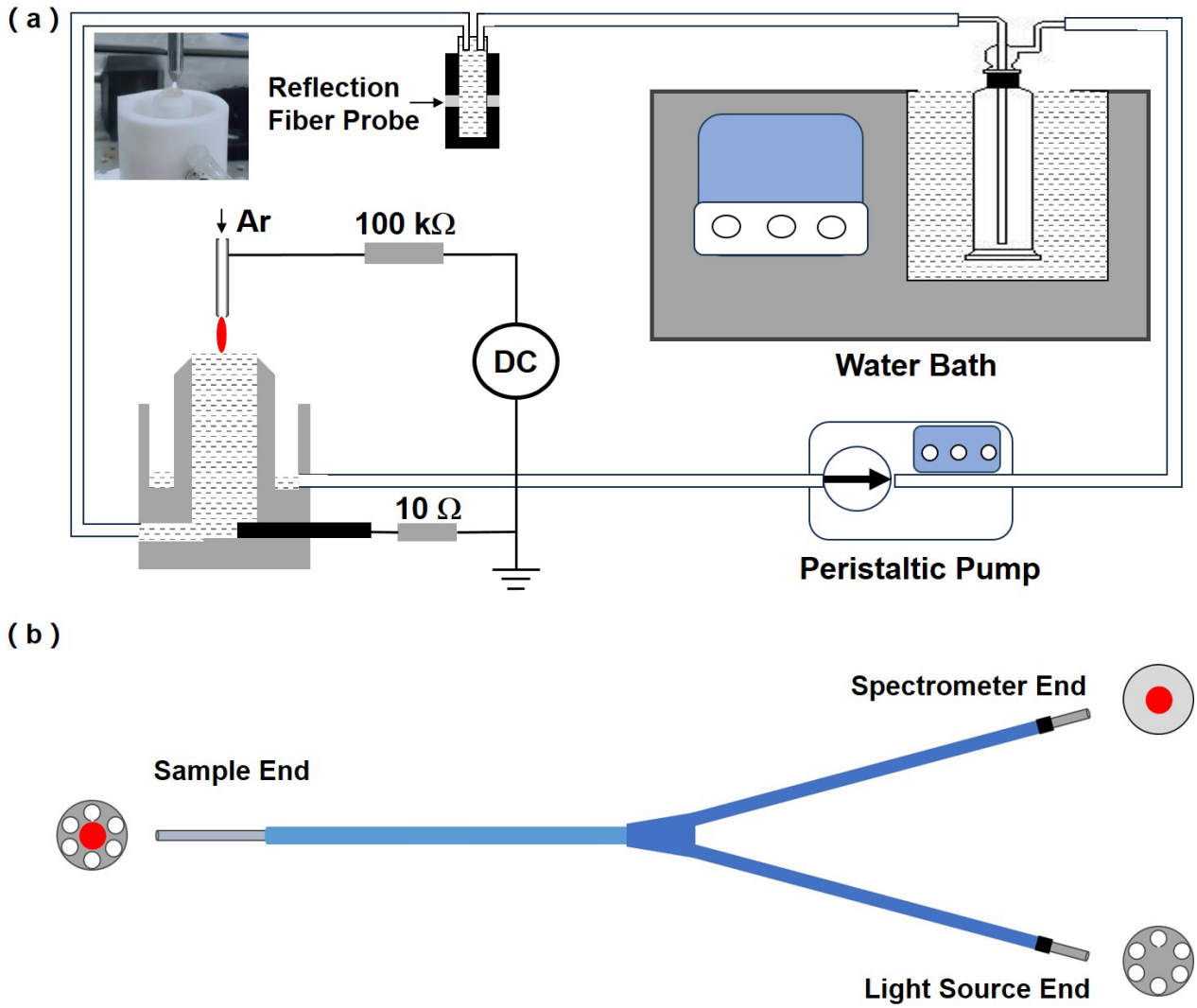

Figure 1. Schematics of (a) the experimental setup, and (b) the reflection optical fiber probe. Inset shows a photograph of the discharge plasma.

3. Results and discussion

Figure 2 shows the fluorescent light intensity of UV-light excited aqueous *HTA* solution as a function of the *HTA* concentration. Using a linear fitting procedure to fit the first 6 points of Fig. 2, the slope of the curve was estimated to be 15.81 μM^{-1}. It is worth noting that the point for 100-μM HTA in Fig. 2 is largely deviated from the linear curve, while it does not affect our results because the HTA concentration we concern in this paper is all in the linear region. Using this value, one can estimate

the quantity of *HTA* generated by the plasma-liquid interactions in the solution.

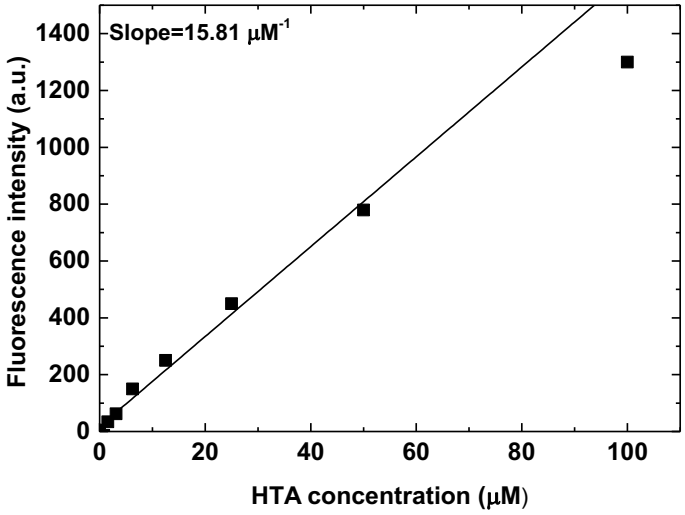

Figure 2. The fluorescent light intensity at the wavelength of 425 nm as a function of the concentration for the UV−light (a LED light source emitted at 310±5 nm) excited aqueous *HTA* solution. A linear fitting gives a slope of the curve being 15.81 μM^{-1}.

Phosphate-buffered aqueous solutions with different *NaTA* concentrations were irradiated by the Ar plasma. By recording the fluorescent light intensity of the plasma-treated solutions, we obtained the *HTA* concentration in the solutions. Using Eq. 11 and 35% for the conversion ratio α[28, 29], one can obtain $[OH]_m$ in the plasma-treated solution. Figure 3 presents the time evolution of the $[OH]_m$ for the plasma-treated solution. One can find that the value of $[OH]_m$ increases rapidly at first, and then its growth rate slowly decreases, especially for solutions with a high *NaTA* concentration. The decrease in the $[OH]_m$ growth rate can be mainly attributed to two factors. First, the consumption of *NaTA* leads to a decrease in the production rate of *HTA* (G_{HTA}) (see Eq. 5). Second, the plasma induced *HTA* decomposition may also cause a decrease in the value of G_{HTA}.

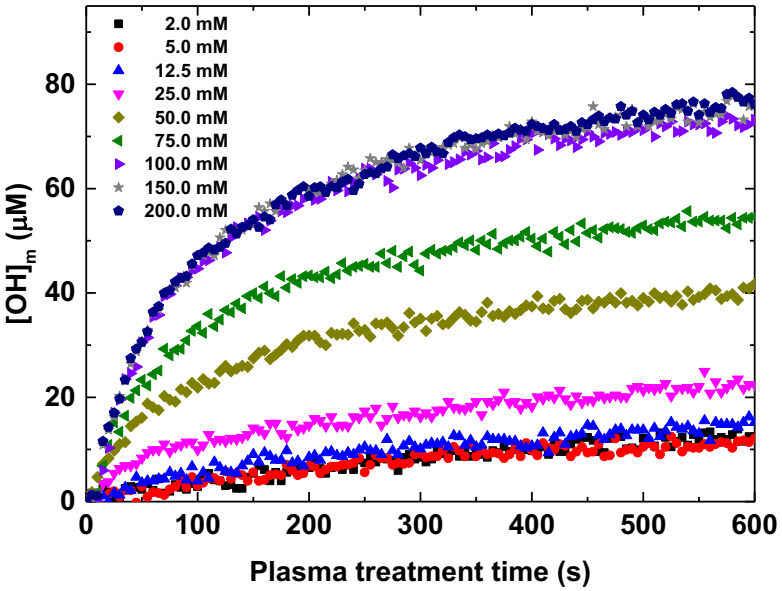

Figure 3. Measured *OH* radical concentraions $\{[OH]_m\}$ as a fucntion of the plasma treatment time in the phosphate-buffered solutions containing different concentrations of *NaTA*.

To obtain a reasonable G_{HTA} without the inference of the *HTA* consumption by plasma-induced decomposition, one should take the derivatives with respect to time for curves of the [*HTA*] *versus* the plasma treatment time at the very beginning of the plasma treatment. Because we recorded the fluorescent light each 5 seconds and the curves are not easy to separate from the very beginning, we choose to calculate the derivatives with respect to time from 0 to 40 sec. Figure 4 shows the reciprocal of the *HTA* production rate as a function of the reciprocal of the *NaTA* concentration in the plasma-treated phosphate-buffered *NaTA* solutions. We found that the value of $1/G_{HTA}$ does not change when the *NaTA* concentration is higher than 100 mM which means almost all generated OH radicals are consumed by the *NaTA* molecules. This result is consistent with the original paper for quantifying *OH* radicals using the fluorescence of *HTA* in Cobalt-60 γ-irradiated aqueous *NaTA* solutions [28]. In addition, our previous work also showed that almost all the *OH* radicals generated from the plasma-liquid interactions were scavenged when the concentration of a *OH* scavenger, dimethylsulfoxide,

was higher than 100 mM [30] (dimethylsulfoxide and *NaTA* have close values of rate constants for interactions with *OH* radicals). All these results imply that $A/[S]$ in Eq. 8 is close to zero as $[NaTA]$ is greater than 100 mM. As discussed in the introduction part, $G_{[OH]g}$ should approximate to $\alpha G_{[HTA]}$ when $[NaTA]$ is greater than 100 mM (if the *OH-HTA* conversion ratio α is concerned).

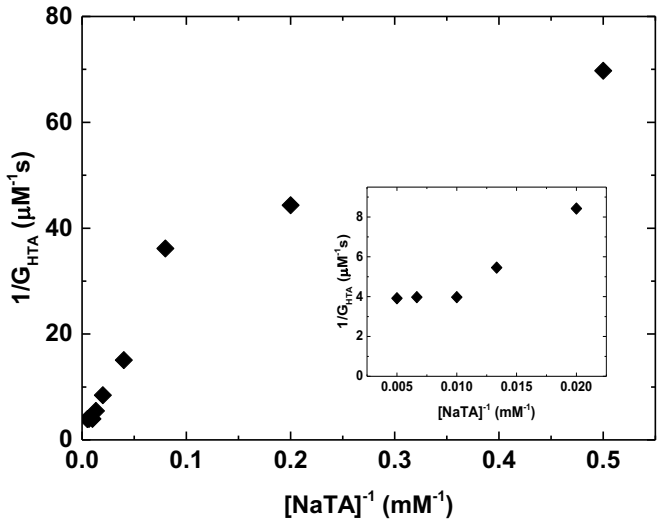

Figure 4. The reciprocal of the *HTA* production rate ($1/G_{HTA}$) as a function of the reciprocal of the NaTA concentration ($1/[NaTA]$)in the plasma-treated phosphate-buffered *NaTA* solutions. Inset shows the enlarged part of the same figure at the small $1/[NaTA]$ zone.

Using Eq. 9 and $G_{[OH]g}= \alpha G_{[HTA]}$ {$[HTA]$=100.0 mM}, one can obtain the concentrations of the plasma-generated *OH* {$[OH]_g$} radicals. Figure 5 presents the time evolutions of the $[HTA]$, $[OH]_m$, and $[OH]_g$ in the plasma-treated *NaTA* solution ($[NaTA]$=100.0 mM). Obviously, the $[OH]_m$ is less than the $[OH]_g$, and the difference between them increases as the plasma treatment becomes longer.

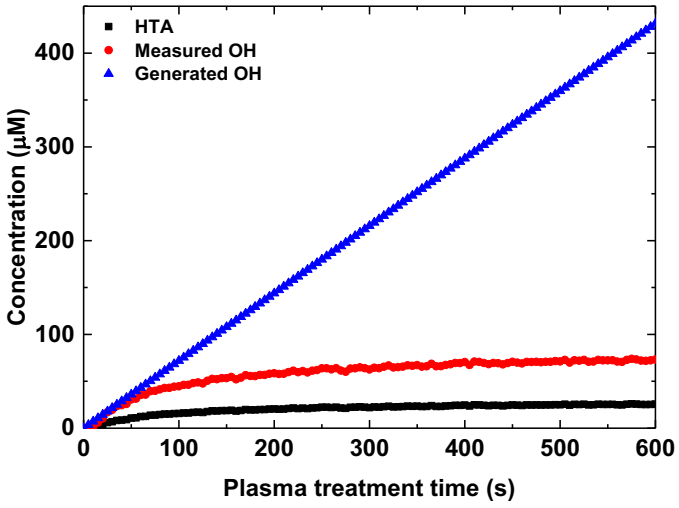

Figure 5. Time evolutions of $[HTA]$, $[OH]_m$, and $[OH]_g$ in the plasma-treated phosphate-buffered *NaTA* solution ($[NaTA]$=100.0 mM).

The discrepancies in Fig. 5 may put the validity of the application of the molecular probe method in the plasma-liquid systems into question. One may ask: what is exactly the $[OH]_m$ and how can we obtain a reasonable plasma-generated *OH* concentration in the plasma-liquid systems? Here we should stress again the concepts dissused in the introduction part. The *OH* radicals generated from the plasma-liquid interactions are consumed through three main channels: the molecular probe, the *OH* species themselves, and the unknown *OH* scavengers, according to Eqs. 1-3. The value of $[OH]_m$ is estimated directly from the process including the molecular probe, and it strongly depends on the factors such as the rate constant between the molecular probe and OH species, and the ratio of concentrations of the molecular probe, *OH* species, and the unknown *OH* scavengers. To measure all the aqueous *OH* (OH_{aq}) radicals generated from the plasma-liquid inteactions, one way is to increase the concentration ratio of molecular probe to other OH consumers so that almost all *OH* species are consumed by the molecular probe. The other way is to choose a molecular probe which can react with the *OH* radicals with a high rate compared with the *OH* species themselves and the unknown *OH*

scavengers. It is well known that the recombination process of *OH* radicals (Eq. 2) has a very large rate constant (5.5×10^9 M^{-1} s^{-1}) [31], and then it is difficult to find a suitable molecular probe with a rate constant several orders greater than this value. Consequently, one should choose the high concentration of molecular probe when using the molecular probe method. We have searched the literatures which used *NaTA* or terephthalic acid (*TA*) as the molecular probe to quantify the OH_{aq} in the plasma-liquid systems, some typical used concentrations of the molecular probe are summarized in Table 3. Besides two recent studies [32, 33], the concentrations of the molecular probe did not exceed 10 mM, and most of them were about 2 mM. Therefore, the previous studies did not use the optimum conentrations for the molecular probe.

Table 3. Typical terephthalic acid (*TA*) or disodium terephthalate (*NaTA*) concentrations used in the fluorescence quantification of *OH* radicals in the plasma-liquid systems.

Molecule probe	Concentration (mM)	References
TA in basic solution	0.2	[29]
TA in basic solution	2	[34-41]
TA (pH=7)	5	[42]
TA in a carbonate buffer or in PBS	10	[43, 44]
TA in basic solution	50	[32]
NaTA	1	[45, 46]
NaTA	2	[47]
NaTA	3	[48]
NaTA	4	[49, 50]
NaTA	20-120	[33]

From the previous analysis and Figs. 3 and 5, we can find that the value of $[OH]_m$ depends on the molecualr probe concentration and the growth rate of $[OH]_m$ gradually decreases with time, while the value $[OH]_g$ linearly increases with the plasma treatment time. Therefore, even when a suitable high conentration is used for the molecular probe, the commonly measured *OH* concetrantion, $[OH]_m$, is still lower than the actual plasma generated *OH* concentration $[OH]_g$ (Fig. 5).

4. Conclusions

The molecular probe diagnostic method is a very useful technique for measuring OH_{aq} radicals

generated through the plasma-liquid interactions. We emphasize that appropriate concentration of the molecular probe is crucial for the *OH* species quantification. Using *NaTA* as the molecular probe, we measured the OH_{aq} concentration in phosphate-buffered solution solutions during Ar plasma treatment. The results indicated that in our case the *NaTA* concentration needs to be higher than 100 mM to obtain a reliable value for the *OH* concentration. If the *NaTA* concentration is less than 100 mM, the measured *OH* concentration is less than the actual one. The presented theoretical analysis is generic and suggests that the results obtained for *NaTA* molecular probe can be extended to other molecular probes. It is crucial to use sufficiently high concentrations of molecular probes for the OH_{aq} quantification in the plasma-liquid systems, which ensure that at least most of the plasma-generated OH_{aq} species will be captured by the used molecular probe. This crucial concentration of the molecular probe is dependent on the types of plasma-liquid systems. By gradually increasing the molecular probe concentration in a plasma-treated liquid system, one can achieve a series of curves of the OH concentrations in the system vs. the plasma treatment time. The sufficient concentration of the used molecular probe for this plasma-liquid system can be determined to be the value above which the curve does not change with the molecular probe concentration. This refined approach allows one to accurately measure the actual concentration of the plasma generated OH_{aq} species, which is required in diverse applications of plasma activated solutions in biomedicine, agriculture, energy and environment, and other fields.

Acknowledgments

This work was partially supported by National Natural Science Foundation of China (Grant Nos.: 52077185 & 61964003).

Data availability statement

All data that support the findings of this study are included within the article.

References

[1] P. K. Chu, X. Lu, Low temperature plasma technology: methods and applications, CRC Press, **2013**.

[2] A. Bogaerts, E. Neyts, R. Gijbels, J. Van der Mullen *Spectrochimica Acta Part B: Atomic Spectroscopy*. **2002**, *57*, 609-658.

[3] C. Richmonds, M. Witzke, B. Bartling, S. W. Lee, J. Wainright, C.-C. Liu, R. M. Sankaran *Journal of the American Chemical Society*. **2011**, *133*, 17582-17585.

[4] P. Rumbach, M. Witzke, R. M. Sankaran, D. B. Go *Journal of the American Chemical Society*. **2013**, *135*, 16264-16267.

[5] P. J. Bruggeman, M. J. Kushner, B. R. Locke, J. G. Gardeniers, W. Graham, D. B. Graves, R. Hofman-Caris, D. Maric, J. P. Reid, E. Ceriani *Plasma Sources Science and Technology*. **2016**, *25*, 053002.

[6] A. Lindsay, C. Anderson, E. Slikboer, S. Shannon, D. Graves *Journal of Physics D: Applied Physics*. **2015**, *48*, 424007.

[7] Q. Chen, T. Kaneko, R. Hatakeyama *Applied Physics Express*. **2012**, *5*, 086201.

[8] T. Kaneko, S. Sasaki, K. Takashima, M. Kanzaki *Journal of clinical biochemistry and nutrition*. **2017**, *60*, 3-11.

[9] D. Liu, Z. Liu, C. Chen, A. Yang, D. Li, M. Rong, H. Chen, M. Kong *Scientific reports*. **2016**, *6*, 23737.

[10] Y. Gorbanev, A. Privat-Maldonado, A. Bogaerts in Analysis of short-lived reactive species in plasma–air–water systems: the dos and the do nots, Vol. (Ed.^Eds.: Editor), ACS Publications, City, **2018**.

[11] V. S. K. Kondeti, C. Q. Phan, K. Wende, H. Jablonowski, U. Gangal, J. L. Granick, R. C. Hunter, P. J. Bruggeman *Free Radical Biology and Medicine*. **2018**, *124*, 275-287.

[12] X.-F. Zhou, H.-F. Xiang, M.-H. Yang, W.-Q. Geng, K. Liu *J. Phys. D: Appl. Phys.* **2023**, *56*, 455202.

[13] B. Locke, M. Sato, P. Sunka, M. Hoffmann, J.-S. Chang *Industrial & Engineering Chemistry Research*. **2006**, *45*, 882-905.

[14] G. R. Stratton, C. L. Bellona, F. Dai, T. M. Holsen, S. M. Thagard *Chemical Engineering Journal*. **2015**, *273*, 543-550.

[15] Y. Yang, Y. I. Cho, A. Fridman, Plasma discharge in liquid: water treatment and applications, CRC press, **2017**.

[16] G. Fridman, G. Friedman, A. Gutsol, A. B. Shekhter, V. N. Vasilets, A. Fridman *Plasma Processes and Polymers*. **2008**, *5*, 503-533.

[17] H. Jablonowski, T. von Woedtke *Clinical Plasma Medicine*. **2015**, *3*, 42-52.

[18] M. G. Kong, G. Kroesen, G. Morfill, T. Nosenko, T. Shimizu, J. Van Dijk, J. Zimmermann *New Journal of Physics*. **2009**, *11*, 115012.

[19] G. Morfill, M. G. Kong, J. Zimmermann *New Journal of Physics*. **2009**, *11*, 115011.

[20] K. Weltmann, T. Von Woedtke *Plasma Physics and Controlled Fusion*. **2016**, *59*, 014031.

[21] K. D. Weltmann, E. Kindel, T. von Woedtke, M. Hähnel, M. Stieber, R. Brandenburg *Pure and Applied Chemistry*. **2010**, *82*, 1223-1237.

[22] A. Wold *Chemistry of Materials*. **1993**, *5*, 280-283.

[23] J. Thomas, J. Rabani, M. Matheson, E. Hart, S. Gordon *The Journal of Physical Chemistry*. **1966**, *70*, 2409-2410.

[24] P. Pagsberg, H. Christensen, J. Rabani, G. Nilsson, J. Fenger, S. O. Nielsen *The Journal of Physical Chemistry*. **1969**, *73*, 1029-1038.

[25] C. Anastasio, B. Matthew *Atmospheric Chemistry and Physics*. **2006**, *6*, 2439-2451.

[26] A. Denaro, P. Owens *Electrochimica Acta*. **1968**, *13*, 157-165.

[27] L. M. Dorfman, G. E. Adams, Reactivity of the hydroxyl radical in aqueous solutions, US Department of Commerce,

National Bureau of Standards Washington, DC, **1973**.
[28] R. W. Matthews *Radiation Research*. **1980**, *83*, 27-41.
[29] S. Kanazawa, H. Kawano, S. Watanabe, T. Furuki, S. Akamine, R. Ichiki, T. Ohkubo, M. Kocik, J. Mizeraczyk *Plasma Sources Science and Technology*. **2011**, *20*, 034010.
[30] X. He, J. Lin, B. He, L. Xu, J. Li, Q. Chen, G. Yue, Q. Xiong, Q. H. Liu *Plasma Sources Science and Technology*. **2018**, *27*, 085010.
[31] G. V. Buxton, C. L. Greenstock, W. P. Helman, A. B. Ross *Journal of physical and chemical reference data*. **1988**, *17*, 513-886.
[32] B. Myers, P. Ranieri, T. Smirnova, P. Hewitt, D. Peterson, M. H. Quesada, E. Lenker, K. Stapelmann *Journal of Physics D: Applied Physics*. **2021**, *54*, 145202.
[33] N. B. Üner, P. Baldaguez Medina, J. L. Dinari, X. Su, R. M. Sankaran *Langmuir*. **2022**, *38*, 8975-8986.
[34] S. Kanazawa, T. Furuki, T. Nakaji, S. Akamine, R. Ichiki *Int. J. Plasma Environ. Sci. Technol*. **2012**, *6*, 166-171.
[35] S. Kanazawa, T. Furuki, T. Nakaji, S. Akamine, R. Ichiki in Application of chemical dosimetry to hydroxyl radical measurement during underwater discharge, Vol. 418 (Ed.^Eds.: Editor), IOP Publishing, City, **2013**, pp.012102.
[36] S. Li, I. Timoshkin, M. Maclean, S. Macgregor, M. Wilson, M. Given, T. Wang, J. Anderson *IEEE Transactions on Dielectrics and electrical insulation*. **2015**, *22*, 1856-1865.
[37] H. Taghvaei, V. Kondeti, P. J. Bruggeman *Plasma Chemistry and Plasma Processing*. **2019**, *39*, 729-749.
[38] H. Hayashi, S. Akamine, R. Ichiki, S. Kanazawa *Int. J. Plasma Environ. Sci. Technol*. **2016**, *10*, 24-28.
[39] S. Lee, J. Lee, W. Nam, G. Yun *Journal of Physics D: Applied Physics*. **2022**, *55*, 455201.
[40] T.-W. Chen, C.-T. Liu, C.-Y. Chen, M.-C. Wu, P.-C. Chien, Y.-C. Cheng, J.-S. Wu *ECS Journal of Solid State Science and Technology*. **2020**, *9*, 115002.
[41] S. Schüttler, L. Jolmes, E. Jeß, K. Tschulik, J. Golda *Plasma Processes and Polymers*. **2023**, e2300079.
[42] F. Tampieri, M.-P. Ginebra, C. Canal *Analytical Chemistry*. **2021**, *93*, 3666-3670.
[43] K. Takeda, S. Sasaki, W. Luo, K. Takashima, T. Kaneko *Applied Physics Express*. **2021**, *14*, 056001.
[44] R. Honda, S. Sasaki, K. Takashima, T. Sato, T. Kaneko *Japanese journal of applied physics*. **2019**, *58*, 106002.
[45] M. Sahni, B. R. Locke *Industrial & Engineering Chemistry Research*. **2006**, *45*, 5819-5825.
[46] K. Ulucan-Altuntas, M. Saleem, G. Tomei, E. Marotta, C. Paradisi *Journal of Environmental Management*. **2022**, *301*, 113885.
[47] K. Ishikawa, M. Sasaki, S. Kumagai *Japanese Journal of Applied Physics*. **2019**, *59*, SAAC11.
[48] P. N. Thanh, T. Sugai, A. Tokuchi, W. Jiang *IEEE Transactions on Plasma Science*. **2022**, *51*, 199-204.
[49] D. Shiraki, N. Ishibashi, N. Takeuchi *IEEE Transactions on Plasma Science*. **2016**, *44*, 3158-3163.
[50] N. Takeuchi, N. Ishibashi *Plasma Sources Science and Technology*. **2018**, *27*, 045010.

Table 1. Notations used in this paper and their meanings.

Notation	Meaning
$[OH]$, $[S]$, $[X]$, $[S^+]$	Steady state concentrations of S, OH, X & S^+
$G_{[OH]g}$	Change rate of the $[OH]$ in the plasma-treated solution, if all dissolved gasoues OH are not consumed
$G_{[S+]}$	Production rate of $[S^+]$ in the solution
$[OH]_g$	Plasma-generated OH in the solution
$[OH]_m$	Measured OH concentration in the plasma-treated solution in most studies

Table 3. Typical terephthalic acid (*TA*) or disodium terephthalate (*NaTA*) concentrations used in the fluorescence quantification of *OH* radicals in the plasma-liquid systems.

Molecule probe	Concentration (mM)	References
TA in basic solution	0.2	[29]
TA in basic solution	2	[34-41]
TA (pH=7)	5	[42]
TA in a carbonate buffer or in PBS	10	[43, 44]
TA in basic solution	50	[32]
NaTA	1	[45, 46]
NaTA	2	[47]
NaTA	3	[48]
NaTA	4	[49, 50]
NaTA	20-120	[33]